PHYSICAL REVIEW D **74,** 064008 (2006)

Quasinormal modes of brane-localized standard model fields. II. Kerr black holes

P. Kanti[*]

Department of Mathematical Sciences, University of Durham Science Site, South Road, Durham DH1 3LE, United Kingdom

R. A. Konoplya[†] and A. Zhidenko[‡]

Instituto de Física, Universidade de São Paulo C.P. 66318, 05315-970, São Paulo-SP, Brazil

(Received 11 July 2006; published 8 September 2006)

This paper presents a comprehensive study of the fundamental quasinormal modes of all standard model fields propagating on a brane embedded in a higher-dimensional rotating black-hole spacetime. The equations of motion for fields with spin $s = 0$, $1/2$ and 1 propagating in the induced-on-the-brane background are solved numerically, and the dependence of their QN spectra on the black-hole angular momentum and dimensionality of spacetime is investigated. It is found that the brane-localized field perturbations are longer-lived when the higher-dimensional black hole rotates faster, while an increase in the number of transverse-to-the-brane dimensions reduces their lifetime. Finally, the quality factor Q, that determines the best oscillator among the different field perturbations, is investigated and found to depend on properties of both the particular field studied (spin, multipole numbers) and the gravitational background (dimensionality, black-hole angular momentum parameter).

DOI: 10.1103/PhysRevD.74.064008 PACS numbers: 04.30.Nk, 04.50.+h

I. INTRODUCTION

The introduction, during the recent years, of gravitational theories that postulate the existence of additional spacelike dimensions in nature [1,2] have radically changed our notion of the universe and of the structure of the spacetime in which we live. The concept of the brane—a $(3 + 1)$-dimensional hypersurface inspired by D-branes encountered in string theory—was introduced, that was embedded in a higher-dimensional spacetime, the bulk. Ordinary Standard Model (SM) particles (scalars, fermions and gauge bosons) are restricted to live on the brane while gravitons can propagate both on and off the brane. In this set-up, the accurately observed properties of SM fields are only marginally altered, nevertheless new effects coming from the embedding of our 4-dimensional world in a higher-dimensional spacetime could still be observed, despite the fact that the bulk itself remains strictly nonaccessible to brane observers.

One such effect could be the creation of microscopic black holes on ground-based accelerators during the collision of highly energetic particles with center-of-mass energy $\sqrt{s} > M_*$ [3], where M_* denotes the fundamental Planck scale of the higher-dimensional gravitational theory. This scenario can be realized in the context of the theory with Large Extra Dimensions [1] that allows for a fundamental gravity scale as low as 1 TeV. As a result, experiments performed at next-generation particle colliders could easily witness effects coming from trans-planckian collisions, such as the creation of microscopic, higher-dimensional black holes that are centered on our brane but extend off the brane as well. The creation of these black holes, and thus the existence of additional dimensions, could be confirmed through the detection of the emitted Hawking radiation which is expected to be their most prominent observable effect [4].

Nevertheless, the creation of these brane black holes might trigger additional observable effects, such as the detection of the spectrum of the so-called quasinormal modes (QNMs) [5,6]. These modes arise as the result of an external perturbation of a black-hole background, either through the addition of a field or by perturbing the metric itself. When this happens, the gravitational system enters a phase of damping oscillations, with the frequency of the field consisting of a real part ω_{Re}, that drives the field oscillations, and of an imaginary part ω_{Im}, that causes the simultaneous damping of these oscillations. Quasinormal modes with small ω_{Im}, and thus long damping time, can dominate the spectrum at very late times after the initial perturbation.

As the detection of the spectrum of QNMs could be considered as direct evidence for the existence of black holes in our universe, a variety of black-hole backgrounds and auxiliary propagating fields have been studied over the years both in 4 dimensions [7] and higher dimensions [8]. Unfortunately, no experimental detection has so far confirmed these theoretical studies. This could be due either to the notorious elusiveness of gravitons or to the fact that simply no black hole exists, as yet, in the vicinity of our neighborhood. If, however, the scenario of the creation of microscopic black holes can be realised at the next-generation colliders, a unique opportunity for detecting the QN spectrum is offered. Since we have not yet successfully detected any gravitons, the obvious candidates would be instead the different species of SM fields that are not only abundant on our brane but also much easier to detect.

[*]Electronic address: panagiota.kanti@durham.ac.uk
[†]Electronic address: konoplya@fma.if.usp.br
[‡]Electronic address: zhidenko@fma.if.usp.br

In [9], we presented a comprehensive study of the QN spectra of all SM fields (scalars, fermions and gauge bosons) living on a 4-dimensional brane, that was embedded in a variety of higher-dimensional, spherically-symmetric black-hole backgrounds. The cases of brane-localized fields propagating in a Schwarzschild, Reissner-Nordström and Schwarzschild-(Anti) de Sitter induced gravitational background were studied in detail, and the effect of various parameters, such as the dimensionality of spacetime, black-hole charge and bulk cosmological constant, on the QN spectra was examined. It was found that an increase in the number of transverse-to-the-brane spacelike dimensions resulted in the faster damping of all fields living on the brane, independently of the exact type of spherically-symmetric projected background. In the presence of a black-hole charge, the QN spectra of all fields resembled more the ones of D-dimensional fields rather than the ones of 4-dimensional, while the presence of a bulk cosmological constant did not lead to significant modifications to the QN spectra compared to the ones of purely 4-dimensional fields. A recent paper [10] follows the same line of research by studying the quasinormal modes of brane-localized black holes and their thermodynamic properties.

In the present work, we extend our previous analysis by considering higher-dimensional black-hole backgrounds with nonvanishing angular momentum. During the high-energy collisions of elementary particles resulting in the creation of black holes, it is unnatural to expect that only head-on collisions, leading to spherically-symmetric black holes, would take place. Collisions with a nonvanishing impact parameter are much more likely to occur, and, in addition, it is for these collisions that the black-hole production cross-section is maximized [3,4]. Therefore, microscopic rotating black holes should be the most generic situation, and the effect of the angular momentum of the black hole on the QN spectra of brane-localized fields needs to be investigated. An earlier paper [11] that appeared in the literature studied the QN spectra of brane-localized SM fields only for the particular case of a 5-dimensional rotating black hole. Here, we extend this work by presenting a comprehensive analysis of the QN spectra of fields with spin $s = 0$, $1/2$ and 1 for arbitrary dimensionality of spacetime and angular momentum of the black hole.

As in our previous analysis, in order to ignore quantum corrections, we will be assuming that the produced black hole has a mass $M_{\rm BH}$ that is at least a few orders of magnitude larger than the fundamental scale of gravity M_*. Also the brane self-energy can be naturally (i.e. in the context of a theory that solves the hierarchy problem) assumed to be of the order of M_*; therefore, it is much smaller than $M_{\rm BH}$, and its effect on the gravitational background can also be ignored.

In Sec. II, we present the theoretical framework for our analysis and the equations of motion for the SM fields propagating in the brane background. Sec. III outlines the numerical techniques employed for the integration of both the radial and angular part of the equation of motion of a field propagating in an axially-symmetric induced background. Our numerical results are presented in Sec. IV, where the effect of the dimensionality of spacetime, angular momentum of the black hole and spin of the particle on the QN spectra is investigated. We finish with your conclusions in Sec. V.

II. MASTER EQUATION FOR PROPAGATION OF FIELDS ON THE BRANE

The line-element describing a higher-dimensional, rotating, neutral black hole is given by the Myers-Perry solution [12]. As mentioned above, in this work we will concentrate on the propagation of SM fields, i.e. fields with spin $s = 0$, $1/2$ and 1, on the induced-on-the-brane gravitational background. This background is given by the projection of the higher-dimensional one onto the brane by fixing the values of the additional angular coordinates that describe the $(D-4)$ extra spacelike dimensions [13,14]. After the projection, the brane background assumes the form [4]

$$ds^2 = \left(1 - \frac{\mu}{\Sigma r^{D-5}}\right)dt^2 + \frac{2a\mu\sin^2\theta}{\Sigma r^{D-5}}dtd\varphi - \frac{\Sigma}{\Delta}dr^2 - \Sigma d\theta^2 - \left(r^2 + a^2 + \frac{a^2\mu\sin^2\theta}{\Sigma r^{D-5}}\right)\sin^2\theta d\varphi^2, \quad (1)$$

where

$$\Delta = r^2 + a^2 - \frac{\mu}{r^{D-5}} \quad \text{and} \quad \Sigma = r^2 + a^2\cos^2\theta. \quad (2)$$

The parameters μ and a are related to the mass and angular momentum, respectively, of the black hole through the definitions [12]

$$M_{\rm BH} = \frac{(D-2)\pi^{(D-1)/2}}{\kappa_D^2\Gamma[(D-1)/2]}\mu, \qquad J = \frac{2}{D-2}M_{\rm BH}a, \quad (3)$$

with $\kappa_D^2 = 8\pi G = 8\pi/M_*^{D-2}$ the D-dimensional Newton's constant. We should note here that the higher-dimensional black hole is assumed to have only one nonvanishing component of angular momentum, about an axis in the brane. This is due to the simplifying assumption that the particles that created the black hole were restricted to live on an infinitely-thin brane [1], therefore, during collision they had a nonvanishing impact parameter only on a 2-dimensional plane along our brane. Also, one should observe that, as in the case of spherically-symmetric black holes, the induced-on-the-brane background has an explicit dependence on the total number of dimensions including the ones transverse to the brane [4].

For the study of the quasinormal modes of all SM fields living on the brane, we need first to derive their equations of motion for propagation in the induced background (1). For this, the following factorized ansatz

$$\Psi_s(t, r, \theta, \varphi) = e^{-i\omega t} e^{im\varphi} \Delta^{-s} P_s(r) S^m_{s,\ell}(\theta), \tag{4}$$

is employed for a field with spin s, where $S^m_{s,\ell}(\theta)$ are the spin-weighted spheroidal harmonics [15]. Then, the use of the Newman-Penrose [16,17] formalism may lead to a "master" equation describing the propagation of all species of SM fields (scalars, fermions and gauge bosons) on the brane. This equation has been derived in [4,18], and, as in the case of a purely 4-dimensional Kerr background [19], it leads to two decoupled equations for the radial

$$\Delta^s \frac{d}{dr}\left(\Delta^{1-s}\frac{dP_s}{dr}\right) + \left(\frac{K^2 - isK\Delta'}{\Delta} + 4is\omega r - \tilde{\lambda}\right)P_s = 0, \tag{5}$$

and angular part

$$\frac{1}{\sin\theta}\frac{d}{d\theta}\left(\sin\theta\frac{dS^m_{s,\ell}}{d\theta}\right) + \left[-\frac{2ms\cos\theta}{\sin\theta} - \frac{m^2}{\sin^2\theta} + a^2\omega^2\cos^2\theta - 2a\omega s\cos\theta + s - s^2\cot^2\theta + \lambda\right]S^m_{s,\ell} = 0, \tag{6}$$

of the field, respectively. In the above, we have used the definitions

$$K = (r^2 + a^2)\omega - am, \qquad \tilde{\lambda} = \lambda + 2s + a^2\omega^2 - 2am\omega. \tag{7}$$

As in 4 dimensions [19], the above equations hold for the upper component $s = |s|$ of all SM fields with spin $s = 0$, $1/2$ and 1, but in this case they describe their propagation not in a purely 4-dimensional background but on a brane embedded in a higher-dimensional Kerr background.

Alternative form: One-dimensional wave equation

As in the case of the study of QNMs of SM fields living on a projected-on-the-brane spherically-symmetric black-hole background [9], we will find it convenient to rewrite the radial Eq. (5) in the form of a one-dimensional Schrödinger (or, wavelike) equation. Here, we generalize both the analysis of [20] performed for the case of a purely 4-dimensional Kerr-like background, as well as the one of [9] where a D-dimensional spherically-symmetric background was projected on the brane. To this end, we define a new radial function and a new ("tortoise") coordinate according to

$$P_s = \rho^{2(s-1/2)} Y_s, \qquad \frac{dr_*}{dr} = \frac{\rho^2}{\Delta}, \tag{8}$$

where

$$\rho^2 = r^2 + a^2 - am/\omega \equiv r^2 + \alpha^2, \tag{9}$$

and the metric function $\Delta(r)$ is given in Eq. (2). Then, Eq. (5) takes the form

$$\left(\frac{d^2}{dr_*^2} + \omega^2\right)Y_s + P\left(\frac{d}{dr_*} + i\omega\right)Y_s - QY_s = 0, \tag{10}$$

where we have defined

$$P = s\left(\frac{4r\Delta}{\rho^4} - \frac{\Delta'}{\rho^2}\right), \tag{11}$$

and

$$Q = \frac{\Delta}{\rho^4}\left\{\tilde{\lambda} - (2s-1)\left[\frac{\Delta}{\rho^2} + (2s-3)\frac{\Delta r^2}{\rho^4} - (s-1)\frac{\Delta' r}{\rho^2}\right]\right\}. \tag{12}$$

By defining further, as in [20],

$$Y_s = hZ_s + 2i\omega\left(\frac{d}{dr_*} - i\omega\right)Z_s, \tag{13}$$

Eq. (10) can now be written as a one-dimensional Schrödinger equation

$$\left(\frac{d^2}{dr_*^2} + \omega^2\right)Z_s = V_s Z_s, \tag{14}$$

with the effective potential V_s given by

$$V_{s=1} = \frac{\Delta}{\rho^4}\left[\tilde{\lambda} - \alpha^2\frac{\Delta}{\rho^4} \mp i\alpha\rho^2\frac{d}{dr}\left(\frac{\Delta}{\rho^4}\right)\right], \tag{15}$$

for spin-1 particles,

$$V_{s=1/2} = \frac{\Delta}{\rho^4}\left[\tilde{\lambda} \mp \rho^2\frac{d}{dr}\left(\frac{\sqrt{\tilde{\lambda}\Delta}}{\rho^2}\right)\right], \tag{16}$$

for spin-$1/2$ particles, and

$$V_{s=0} = \frac{\Delta}{\rho^4}\left[\tilde{\lambda} + \frac{\Delta}{\rho^2} - \frac{3\Delta r^2}{\rho^4} + \frac{\Delta' r}{\rho^2}\right], \tag{17}$$

for spin-0 particles. The QN modes for gauge bosons, fermions and scalars living on the brane in the vicinity of a Kerr-like induced background can be found by solving Eq. (14) upon choosing the appropriate effective potential. Here, we will undertake this task and compute the QNMs of brane-localized SM fields through numerical analysis—the details of it are explained in the next section and our results are presented in the following one.

III. NUMERICAL ANALYSIS

In order to calculate the QNMs of brane-localized fields, we need to solve the radial Eq. (5), or its equivalent form (14). To this end, we need the expression of the angular eigenvalue λ, that appears in the radial equation. For a vanishing black-hole angular momentum, i.e. $a = 0$, the angular eigenvalue is simply given by $\lambda = \ell(\ell+1) - s(s+1)$, where $\ell = s, s+1, s+2\ldots$ are (half)integer numbers; therefore, the angular equation can be altogether ignored for the purpose of calculating QN modes. However, in the case of an axially-symmetric black-hole

background, the angular eigenvalue cannot be written in a closed form, and its exact value can be found only numerically [21] by using the angular Eq. (6).

For $a \neq 0$, the spectrum of λ for a given value of ω is a set of complex numbers that cannot be easily put into correspondence with a set of angular numbers ℓ. In order to find the exact value of $\lambda(\omega)$, and at the same time the solution to Eqs. (5) and (6), we follow a technique inspired by perturbation theory: we start with the known solution of the angular equation for $a = 0$ (i.e. with the spin-weighted spherical harmonics), and increase a by a small amount; then, for a given energy ω, we search for the solution of Eqs. (5) and (6) that is regular and closest to the original one; this solution is characterized by a unique value $\lambda(\omega)$. By repeating the same analysis for different values of (a, ω), the spectrum of $\lambda(\omega)$, as well as the solution to the radial and angular equations, can be found for a wide range of the angular momentum parameter a.

The quasinormal modes follow from the numerical integration of the radial Eq. (5) after imposing the following boundary conditions [5,6]

$$P_s \simeq C_+ \exp(i\omega r)/r, \quad \text{as } r \to \infty, \tag{18}$$

$$P_s \simeq C_-(r - r_h)^{-i\kappa}, \quad \text{as } r \to r_h, \tag{19}$$

where

$$\kappa = \frac{\omega r_h(r_h^2 + a^2) - mar_h}{(n-1)(r_h^2 + a^2) + 2r_h^2}, \tag{20}$$

and thus correspond to outgoing waves at spatial infinity and to ingoing waves at the event horizon r_h. The black-hole horizon is derived by solving the equation $\Delta(r) = 0$. Unlike the $4D$ Kerr black hole for which there is an inner and outer solution for r_h, for $D \geq 5$ there is only one real, positive solution to this equation, satisfying the relation $r_h^{D-3} = \mu/(1 + a_*^2)$, where we have defined $a_* = a/r_h$.

The radial Eq. (5) can be solved by using the continued fraction method [22]. For this, the remaining regular singular points of Eq. (5) need to be identified. For $D = 5$, there is only one more singularity at $r = -r_h$. That is why the Frobenius series has a form similar to the one of the ordinary 4-dimensional Kerr background

$$P_s(r) = \frac{\exp(i\omega r)}{r + r_h}\left(\frac{r - r_h}{r + r_h}\right)^{-i\kappa} \sum_{i=0}^{\infty} b_i \left(\frac{r - r_h}{r + r_h}\right)^i. \tag{21}$$

For $D > 5$, there are $D - 3$ additional singularities, one of them being at $r = 0$. Fortunately, for $D \leq 9$, $|1 - r_h/r| > 1$ for all of them, thus the appropriate Frobenius series in this case has the following form

$$P_s(r) = \frac{\exp(i\omega r)}{r}\left(1 - \frac{r_h}{r}\right)^{-i\kappa} \sum_{i=0}^{\infty} b_i \left(1 - \frac{r_h}{r}\right)^i. \tag{22}$$

For $D > 9$, some of the singularities appear in the unit circle and one has to continue the Frobenius series through some midpoints. This technique was recently developed in [23].

Substituting the above series into Eq. (5), one can obtain a $(2D - 5)$-term relation for the coefficients b_i

$$\sum_{j=0}^{\min(2D-6,i)} c_{j,i}^{(2D-5)}(\omega, \lambda) b_{i-j} = 0, \quad \text{for } i > 0. \tag{23}$$

Each of the functions $c_{j,i}^{(2D-5)}(\omega, \lambda)$ has an analytical form in terms of s, i, ω and λ, for a specific dimensionality D and each integer $0 \leq j \leq 2D - 6$.

We now decrease by one the number of terms in the relation

$$\sum_{j=0}^{\min(k,i)} c_{j,i}^{(k+1)}(\omega, \lambda) b_{i-j} = 0, \tag{24}$$

i.e. find the $c_{j,i}^{(k)}(\omega, \lambda)$ that satisfy the equation

$$\sum_{j=0}^{\min(k-1,i)} c_{j,i}^{(k)}(\omega, \lambda) b_{i-j} = 0. \tag{25}$$

For $i \geq k$, we can rewrite the above as

$$\frac{c_{k,i}^{(k+1)}(\omega, \lambda)}{c_{k-1,i-1}^{(k)}(\omega, \lambda)} \sum_{j=1}^{k} c_{j-1,i-1}^{(k)}(\omega, \lambda) b_{i-j} = 0. \tag{26}$$

Subtracting (26) from (24) we find the relation (25) explicitly, thus we obtain:

$$c_{j,i}^{(k)}(\omega, \lambda) = c_{j,i}^{(k+1)}(\omega, \lambda), \quad \text{for } j = 0, \quad \text{or} \quad i < k,$$

$$c_{j,i}^{(k)}(\omega, \lambda) = c_{j,i}^{(k+1)}(\omega, \lambda) - \frac{c_{k,i}^{(k+1)}(\omega, \lambda) c_{j-1,i-1}^{(k)}(\omega, \lambda)}{c_{k-1,i-1}^{(k)}(\omega, \lambda)},$$

otherwise. This procedure is called *Gaussian eliminations*, and allows us to determine numerically the coefficients in the three-term relation

$$c_{0,i}^{(3)} b_i + c_{1,i}^{(3)} b_{i-1} + c_{2,i}^{(3)} b_{i-2} = 0, \quad \text{for } i > 1$$
$$c_{0,1}^{(3)} b_1 + c_{1,1}^{(3)} b_0 = 0, \tag{27}$$

for given ω (and therefore λ) up to any finite i. The complexity of the procedure is *linear* with respect to i and k.

The requirement that the Frobenius series be convergent at spatial infinity implies that

$$0 = c_{1,1}^{(3)} - \frac{c_{0,1}^{(3)} c_{2,2}^{(3)}}{c_{1,2}^{(3)} -} \frac{c_{0,2}^{(3)} c_{2,3}^{(3)}}{c_{1,3}^{(3)} -} \ldots. \tag{28}$$

The above can be inverted N times to give

$$c^{(3)}_{1,N+1} - \frac{c^{(3)}_{2,N}c^{(3)}_{0,N-1}}{c^{(3)}_{1,N-1}-}\frac{c^{(3)}_{2,N-1}c^{(3)}_{0,N-2}}{c^{(3)}_{1,N-2}-}\cdots\frac{c^{(3)}_{2,2}c^{(3)}_{0,1}}{c^{(3)}_{1,1}} = \frac{c^{(3)}_{0,N+1}c^{(3)}_{2,N+2}}{c^{(3)}_{1,N+2}-}\frac{c^{(3)}_{0,N+2}c^{(3)}_{2,N+3}}{c^{(3)}_{1,N+3}-}\cdots. \quad (29)$$

This equation with *infinite continued fraction* on the right-hand side can be solved numerically by minimizing the absolute value of the difference between the left- and right-hand sides. The equation has an infinite number of roots (corresponding to the QN spectrum), but for each N the most stable root is different. In general, we have to use the N times inverted equation to find the N-th QN mode. The requirement that the continued fraction be itself convergent allows us to limit its depth by some large value, always ensuring that an increase in this value does not change the final results within the desired precision. To check the correctness of the obtained results we compared them with those obtained in [9] with the help of WKB method [24]. The WKB method is known to give very accurate results for higher values of ℓ [25].

The complete numerical code for determining the QN spectrum was written in MATHEMATICA®, and is available from the last author upon request.

IV. NUMERICAL RESULTS

We now proceed to the presentation of our numerical results for the QN spectra of brane-localized fields with spin $s = 0, 1/2$ and 1 living on a higher-dimensional Kerr black-hole induced background. In what follows, we discuss separately each species of fields and the dependence of its QN spectrum on the angular momentum of the black hole for arbitrary dimensionality of spacetime.

TABLE I. QN frequencies ωr_h for scalar fields, for the mode $\ell = 0$, $m = 0$ and various values of the BH angular momentum $a_* \equiv a/r_h$ and bulk dimensionality D.

a_*	$D = 5$	$D = 6$	$D = 7$
0.0	0.27339–0.41091i	0.21040–0.57167i	0.07281–0.61990i
0.5	0.24918–0.35635i	0.18233–0.51895i	0.04666–0.54481i
1.0	0.19904–0.26464i	0.12312–0.42301i	0.01619–0.40662i
1.5	0.15277–0.19716i	0.06734–0.33503i	–
2.0	0.11874–0.15493i	0.03337–0.26202i	–
2.5	0.09556–0.12834i	0.01790–0.20889i	–
3.0	0.08032–0.11010i	0.01081–0.17195i	–
3.5	0.06978–0.09604i	–	–
4.0	0.06167–0.08478i	–	–
4.5	0.05513–0.07574i	–	–
5.0	0.04978–0.06843i	–	–
5.5	0.04536–0.06241i	–	–
6.0	0.04166–0.05736i	–	–

A. Brane-localized scalar fields

Starting with the case of brane fields with spin $s = 0$, in Table I we display the fundamental modes ($n = 0$) of the QN spectrum for the partial mode ($\ell = 0$, $m = 0$). Throughout this paper, unless explicitly stated, we will be focusing on the fundamental modes of the spectrum as they are found to dominate the signal, with the contribution of the second mode coming out to be about 1%, and that of the higher overtones even smaller. In Table I, the quasinormal frequencies for the scalar field are presented in terms of the angular momentum of the black hole, measured in units of the black-hole horizon radius r_h, and for the values $D = 5$, 6 and 7 of the dimensionality of spacetime—note that an upper bound exists on the value of the angular momentum parameter of the black hole given by $a_*^{\max} = (D-2)/2$ [26] and following from the assumption that the black hole was created by the collision of two particles with impact parameter $b < r_h$; nevertheless, for completeness, here we extend our analysis to higher values of a_* thus allowing for black holes created by alternative mechanisms. From the entries of Table I, one easily observes that, as a_* increases, both the real and imaginary part of the QN frequency decreases. The latter feature makes the damping time longer and the field oscillations on the brane longer-lived. On the other hand, for fixed a_* and variable D, we find the same behavior as in the case of a nonrotating black hole [9] with the real part of the QN frequency being suppressed and the imaginary part enhanced, as D increases.

As the reader notes, the study of the mode ($\ell = 0$, $m = 0$) is incomplete; this is due to the very slow convergence of the Frobenius procedure for this particular mode as D and a become large. Although upon allowing sufficient computing time the missing quasinormal modes could be found, the timescale for doing so does come out to be unrealistically large. For this reason, in Table II we present detailed numerical results for the next partial mode ($\ell = 1$, $m = 0$). These results confirm the monotonic suppression of both the real and imaginary part of the quasinormal frequency, as a_* increases, thus pointing to the conclusion that this behavior is independent of the particular multipole number. In addition, the more complete display of results available for this mode reveal some additional features of the spectrum. To start with, the increase in $\omega_{\rm Re}$ found in [9] for the mode ($\ell = 1$, $m = 0$) as D goes from 5 to 6 is actually followed by a decrease as D increases further, with this behavior persisting for all values of a_*; on the other hand, the behavior of $\omega_{\rm Im}$ continues to be monotonically increasing as D takes larger values.

One additional important feature emerging from the entries of Table II is the existence of asymptotic values for both $\omega_{\rm Re}$ and $\omega_{\rm Im}$, as $a_* \to \infty$. These asymptotic values appear for all values of D, and for all scalar modes. In Fig. 1, we display the QN spectra for the scalar modes ($\ell = 1$, $m = -1, 0, 1$) as a function of the black-hole angular

TABLE II. QN frequencies ωr_h for scalar fields, for the mode $\ell = 1$, $m = 0$ and various values of the BH angular momentum $a_* \equiv a/r_h$ and bulk dimensionality D.

a_*	$D = 5$	$D = 6$	$D = 7$	$D = 8$	$D = 9$
0.0	0.75085–0.36387i	0.81265–0.50454i	0.81678–0.61105i	0.79233–0.68002i	0.76177–0.71730i
0.5	0.68028–0.31425i	0.74928–0.45732i	0.75414–0.56410i	0.72911–0.63029i	0.69952–0.66372i
1.0	0.54711–0.23270i	0.62853–0.37640i	0.63235–0.48047i	0.60568–0.53769i	0.57925–0.56198i
1.5	0.43282–0.17331i	0.52186–0.31276i	0.52101–0.40993i	0.49343–0.45466i	0.47184–0.46989i
2.0	0.35010–0.13527i	0.44102–0.26836i	0.43401–0.35623i	0.40757–0.38891i	0.39096–0.39791i
2.5	0.29112–0.11016i	0.38023–0.23672i	0.36761–0.31440i	0.34386–0.33751i	0.33138–0.34279i
3.0	0.24803–0.09267i	0.33336–0.21315i	0.31655–0.28076i	0.29609–0.29694i	0.28670–0.30011i
3.5	0.21554–0.07987i	0.29619–0.19478i	0.27671–0.25307i	0.25944–0.26447i	0.25230–0.26642i
4.0	0.19033–0.07013i	0.26599–0.17991i	0.24510–0.22993i	0.23065–0.23807i	0.22512–0.23930i
4.5	0.17025–0.06249i	0.24096–0.16751i	0.21961–0.21035i	0.20751–0.21627i	0.20317–0.21707i
5.0	0.15392–0.05633i	0.21988–0.15690i	0.19873–0.19364i	0.18856–0.19802i	0.18508–0.19854i
5.5	0.14041–0.05128i	0.20190–0.14766i	0.18136–0.17925i	0.17276–0.18254i	0.16994–0.18289i
6.0	0.12904–0.04705i	0.18640–0.13950i	0.16672–0.16675i	0.15940–0.16926i	0.15708–0.16951i

momentum parameter a_*, for fixed dimensionality ($D = 5$). The presence of asymptotic values for both ω_{Re} and ω_{Im} for all modes is obvious. Coming back to the entries of Table II, one may observe the potential existence of an asymptotic value for the imaginary part of the QN frequency also as D adopts large values: although ω_{Im} clearly follows an increasing pattern, the step becomes gradually smaller as D increases—we will return to this point later on.

Finally, a point to be addressed is the quality factor of the black hole as an oscillator, defined by

$$Q \sim \frac{1}{2}\frac{\omega_{\mathrm{Re}}}{|\omega_{\mathrm{Im}}|}. \tag{30}$$

The larger the above factor is, the better oscillator the corresponding field is. We find that the quality factor for scalar fields has a distinctly different behavior for different values of D: in the case of $D = 5$ there is a monotonic increase of the quality factor Q, as a function of the rotation parameter a, that renders the scalar fields better oscillators as the black-hole rotates faster. However, as D increases, the increase in Q is soon followed by a suppression, and, for large enough values of D, Q is monotonically decreasing. This behavior is depicted in Fig. 2 for the scalar mode ($\ell = 1$, $m = 0$). Although, in principle, the exact value of the quality factor is determined by all parameters of the black hole (M_{BH}, a) and of the propagating field (s, ℓ, m, n), it seems that, in the case of scalar fields and of the lower multipole modes, there are two main rival factors: the angular momentum of the black hole, that tends to increase Q, and the spacetime dimensionality, that tends to decrease it. As is evident from Fig. 2, in all cases, the quality factor reaches an asymptotic constant value as $a_* \to \infty$, in agreement with the discussion above.

B. Brane-localized gauge bosons

We now turn to the case of gauge fields propagating in the induced-on-the-brane background of a higher-dimensional rotating black hole. Our results are displayed in Table III, and similarly to the case of scalar fields, they

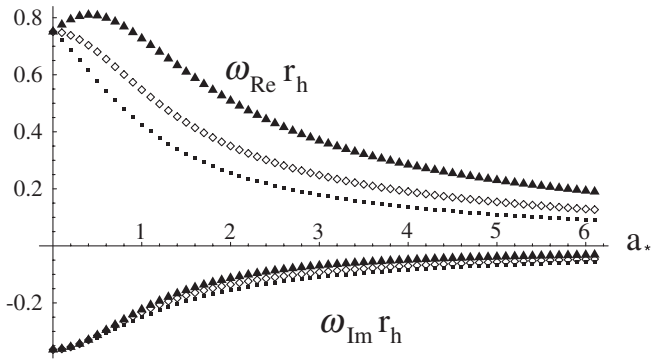

FIG. 1. Fundamental QN frequencies of a scalar field, as a function of a_*, for the multipole mode $\ell = 1$, spacetime dimensionality $D = 5$, and $m = 1$, 0, -1 (depicted by triangles, rhombuses and squares, respectively).

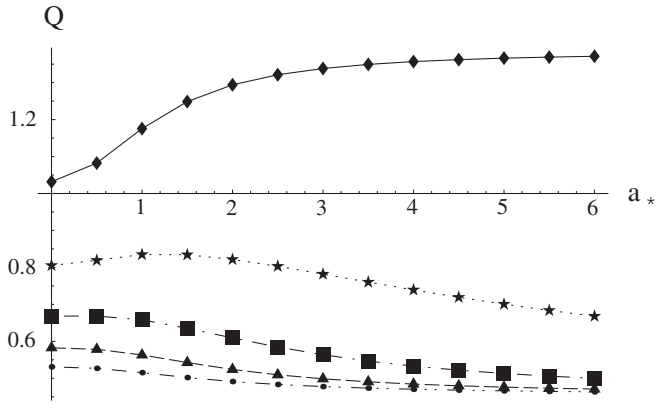

FIG. 2. Quality factor for the scalar field multipole mode ($\ell = 1$, $m = 0$), and for $D = 5, 6, \ldots 9$ (from top to bottom).

TABLE III. QN frequencies ωr_h for gauge fields, for the mode $\ell = 1$, $m = 0$ and various values of the BH angular momentum $a_* \equiv a/r_h$ and bulk dimensionality D.

a_*	$D = 5$	$D = 6$	$D = 7$	$D = 8$	$D = 9$
0.0	0.57667–0.31749i	0.58397–0.40214i	0.56925–0.44900i	0.55266–0.47270i	0.53963–0.48451i
0.5	0.52746–0.27360i	0.54068–0.36152i	0.52762–0.40874i	0.51222–0.43168i	0.50037–0.44273i
1.0	0.43057–0.20043i	0.45531–0.29121i	0.44497–0.33654i	0.43206–0.35645i	0.42276–0.36532i
1.5	0.34379–0.14693i	0.37737–0.23574i	0.36855–0.27619i	0.35810–0.29186i	0.35125–0.29827i
2.0	0.27931–0.11307i	0.31725–0.19716i	0.30905–0.23173i	0.30067–0.24357i	0.29569–0.24807i
2.5	0.23272–0.09115i	0.27183–0.16975i	0.26399–0.19877i	0.25728–0.20768i	0.25363–0.21086i
3.0	0.19845–0.07615i	0.23694–0.14938i	0.22949–0.17365i	0.22410–0.18042i	0.22137–0.18273i
3.5	0.17253–0.06533i	0.20952–0.13360i	0.20255–0.15396i	0.19817–0.15919i	0.19609–0.16091i
4.0	0.15238–0.05718i	0.18751–0.12096i	0.18105–0.13815i	0.17746–0.14227i	0.17584–0.14358i
4.5	0.13633–0.05083i	0.16950–0.11058i	0.16356–0.12521i	0.16058–0.12851i	0.15931–0.12952i
5.0	0.12327–0.04575i	0.15453–0.10187i	0.14908–0.11443i	0.14659–0.11712i	0.14557–0.11792i
5.5	0.11245–0.04159i	0.14190–0.09445i	0.13693–0.10532i	0.13482–0.10754i	0.13399–0.10818i
6.0	0.10335–0.03812i	0.13113–0.08804i	0.12658–0.09753i	0.12478–0.09939i	0.12409–0.09991i

reveal the monotonic suppression of both the real and imaginary part of the QN frequency, as the angular momentum of the black hole increases. In addition, as $a_* \to \infty$, constant asymptotic values emerge for both $\omega_{\rm Re}$ and $\omega_{\rm Im}$ of the quasinormal frequency. This is obvious from the results displayed in Table III for the mode ($\ell = 1$, $m = 0$), but it has been found to hold also for the modes $m = \pm 1$.

When a_* is kept fixed while D varies, $\omega_{\rm Re}$ first increases as D goes from 5 to 6, in accordance with the generic behavior found in [9], but as D increases further, a monotonic suppression takes over again. Also in agreement with the nonrotating case [9], the imaginary part of the QN frequency monotonically increases, as D grows, making the gauge field perturbations shorter-lived. The existence of a potential asymptotic value for $\omega_{\rm Im}$, as $D \to \infty$, can again be inferred from the entries of Table III.

The quality factor Q for gauge bosons is again strongly dependent on the value of the dimensionality of spacetime D. Its behavior for the mode ($\ell = 1$, $m = 0$) and for the values $D = 5, 6, \ldots, 9$ is shown in Fig. 3. As is obvious, for $D = 5$ we obtain again a sharp monotonic increase, as a_* increases. For $D = 6$, 7, we find, as in the case of scalar fields, a nonmonotonic behavior with an initial increase followed by a decrease. The deviation from the case of scalar fields arises for $D > 7$, where the monotonic suppression found in that case gives its place to a monotonic enhancement, although a marginal one.

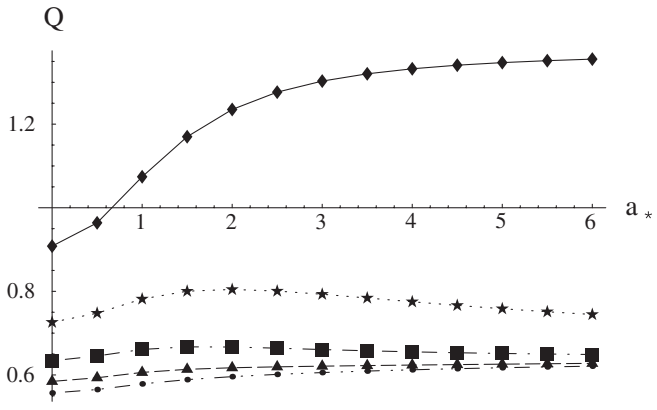

FIG. 3. Quality factor for the gauge field multipole mode ($\ell = 1$, $m = 0$), and for $D = 5, 6, \ldots 9$ (from top to bottom).

C. Brane-localized fermions

We finally address the case of brane-localized spinor fields. In Tables IV and V, we present results for the two lowest multipole modes ($\ell = 1/2$, $m = 1/2$) and ($\ell = 1/2$, $m = -1/2$), respectively, for various values of the black-hole angular momentum parameter and dimensionality of spacetime. Unlike the previously studied cases of scalars and gauge fields, a deviation is observed in the behavior of these two modes, therefore we discuss both of them here separately.

Starting from the mode ($\ell = 1/2$, $m = 1/2$), whose QN spectrum is presented in Table IV, we find that, in terms of a_*, the generic behavior noticed for the other two species of fields also prevails here: both $\omega_{\rm Re}$ and $\omega_{\rm Im}$ monotonically decrease as the angular momentum of the black-hole increases, eventually reaching constant asymptotic values. On the other hand, for fixed a_* and variable D, $\omega_{\rm Im}$ increases monotonically, as for the other two species of fields, with the only difference being the absence of an asymptotic value as $D \to \infty$. A further deviation arises in the dependence of $\omega_{\rm Re}$ on D with its exact behavior depending on the value of the black-hole angular momentum: for low values of a_*, $\omega_{\rm Re}$ follows the traditional increase-followed-by-a-decrease pattern, while for high values of a_* a monotonic decrease for all values of D is observed instead.

Turning to the mode ($\ell = 1/2$, $m = -1/2$) and to the entries of Table V, the deviation in the behavior of its QN spectrum is even more striking. As a_* increases, its $\omega_{\rm Re}$ and $\omega_{\rm Im}$ monotonically decrease towards some constant

TABLE IV. QN frequencies ωr_h for spinor fields, for the mode $\ell = 1/2$, $m = 1/2$ and various values of the BH angular momentum $a_* \equiv a/r_h$ and bulk dimensionality D.

a_*	$D = 5$	$D = 6$	$D = 7$	$D = 8$	$D = 9$
0.0	0.44130–0.35984i	0.45332–0.51049i	0.41925–0.65204i	0.33208–0.78624i	0.31438–1.28297i
0.5	0.45308–0.29340i	0.45965–0.43444i	0.41755–0.55905i	0.32135–0.65497i	0.30694–1.11216i
1.0	0.39498–0.19854i	0.40166–0.33780i	0.34902–0.44834i	0.25178–0.49810i	0.23566–0.95459i
1.5	0.32503–0.13271i	0.33293–0.27005i	0.27090–0.36141i	0.19483–0.37575i	0.18243–0.85971i
2.0	0.26747–0.09332i	0.27517–0.22679i	0.20951–0.29541i	0.15719–0.29478i	0.14483–0.80778i
2.5	0.22380–0.06941i	0.22978–0.19751i	0.16694–0.24551i	0.13128–0.24071i	0.11788–0.77704i
3.0	0.19081–0.05414i	0.19420–0.17589i	0.13772–0.20815i	0.11251–0.20284i	0.09839–0.75720i
3.5	0.16548–0.04387i	0.16604–0.15868i	0.11695–0.17989i	0.09836–0.17507i	0.08409–0.74360i
4.0	0.14561–0.03665i	0.14356–0.14430i	0.10155–0.15807i	0.08734–0.15390i	0.07332–0.73388i
4.5	0.12969–0.03137i	0.12551–0.13196i	0.08972–0.14082i	0.07852–0.13726i	0.06498–0.72671i
5.0	0.11671–0.02740i	0.11091–0.12125i	0.08036–0.12689i	0.07131–0.12386i	0.05835–0.72126i
5.5	0.10594–0.02433i	0.09900–0.11190i	0.07277–0.11543i	0.06531–0.11283i	0.05296–0.71701i
6.0	0.09688–0.02192i	0.08918–0.10371i	0.06649–0.10585i	0.06024–0.10360i	0.04849–0.71363i

asymptotic values, as expected, only for the values $D = (5, 6)$. As D increases further, the initial phase of decrease for ω_{Re} follows a phase of enhancement; ω_{Im} behaves even more singularly by oscillating for $D = 7$ and monotonically increasing for $D \geq 8$. When a_* is kept fixed and D varies, the previously observed behavior is followed only for low values of a_*, with ω_{Re} increasing until $D = 6$ and decreasing for greater values of D; for values of the angular momentum parameter higher than $a_* = 3$, the enhancement phase is extended at least up to $D = 7$. Finally, ω_{Im} follows the traditional increasing pattern with D, however, as in the case of $m = 1/2$, there is no sign for the existence of an asymptotic value as $D \to \infty$.

The alert reader might have noticed that the deviations in the behavior of the QN spectrum for the aforementioned spinor modes arise in the case of either large a_* or large D. In Sec. IV A. we commented on the very slow convergence of the Frobenius procedure, for exactly these ranges of parameters, that failed to give us complete results for the lowest scalar mode ($\ell = 0$, $m = 0$). The same problem appeared also in the case of the spinor mode ($\ell = 1/2$, $m = -1/2$), as it is obvious from Table V. Although numerical results were successfully derived for smaller values of either a_* and/or D, it might be possible that the looming bad convergence behavior of our numerical method contaminated these results, too. Another reason for the observed modifications might be the fact that the equations for the QN modes corresponding to different ℓ's are entangled and, at times, it is extremely difficult to distinguish QN modes by their multipole number, especially in the case of ultraspinning black holes. For the above reasons, the determined results for spinor fields for high values of either a_* or D should be taken with caution.

Finally, the quality factor for the spinor field mode ($\ell = 1/2$, $m = 1/2$) closely follows the behavior observed in the case of scalar and gauge fields, as it is obvious from Fig. 4. For $D = 5$, Q has a monotonically increasing dependence on a_*, that brings it to a value higher than

TABLE V. QN frequencies ωr_h for spinor fields, for the mode $\ell = 1/2, m = -1/2$ and various values of the BH angular momentum $a_* \equiv a/r_h$ and bulk dimensionality D.

a_*	$D = 5$	$D = 6$	$D = 7$	$D = 8$	$D = 9$
0.0	0.44130–0.35984i	0.45332–0.51049i	0.41925–0.65204i	0.33208–0.78624i	0.31438–1.28297i
0.5	0.35706–0.32705i	0.37986–0.49522i	0.34876–0.66241i	0.25678–0.84279i	0.17791–1.40707i
1.0	0.26937–0.25567i	0.30417–0.43439i	0.27267–0.63077i	0.17717–0.87878i	0.04019–1.48580i
1.5	0.20663–0.19865i	0.25106–0.37925i	0.21963–0.60756i	0.14808–0.92662i	–
2.0	0.16466–0.15934i	0.21607–0.33850i	0.18960–0.60173i	0.16145–0.97336i	–
2.5	0.13587–0.13196i	0.19246–0.30939i	0.17898–0.60691i	–	–
3.0	0.11525–0.11217i	0.17585–0.28853i	0.18277–0.61502i	–	–
3.5	0.09988–0.09735i	0.16372–0.27344i	0.19531–0.62133i	–	–
4.0	0.08804–0.08588i	0.15462–0.26239i	0.21210–0.62451i	–	–
4.5	0.07865–0.07678i	0.14768–0.25420i	0.23044–0.62496i	–	–
5.0	0.07105–0.06939i	0.14236–0.24804i	0.24898–0.62352i	–	–
5.5	0.06477–0.06327i	0.13830–0.24332i	–	–	–
6.0	0.05949–0.05814i	0.13527–0.23962i	–	–	–

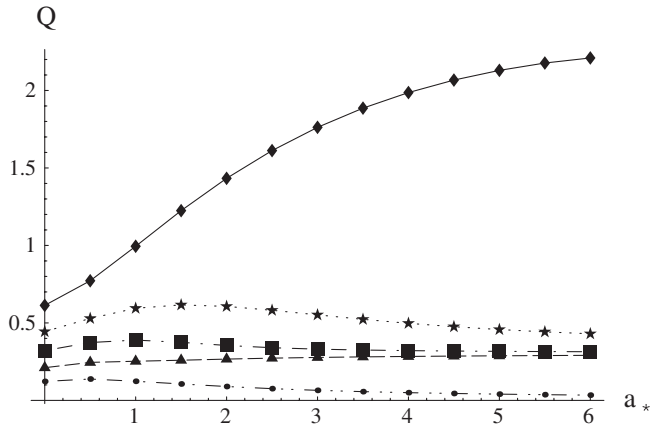

FIG. 4. Quality factor for the spinor field multipole mode ($\ell = 1/2$, $m = 1/2$), and for $D = 5, 6, \ldots 9$ (from top to bottom).

for other species, thus rendering the fermions the best oscillators among the lowest multipole modes. For $D \geq 6$, the quality factor reaches a maximum value and then follows a decreasing pattern; for large values of D, the change in the value of Q, as a_* varies, is only marginal. Turning to the mode ($\ell = 1/2, m = -1/2$), we may easily see from Fig. 5 that the quality factor follows a radically different behavior. Although the suppression with the dimensionality of spacetime is still present, the enhancement in terms of a_* has disappeared. For $D = (5, 6)$, we can observe a monotonic decrease in Q, as a_* grows, while for $D = 7$ the decrease in Q changes to an increase, after reaching a minimum at $a_* \approx 2.5$. The absence of robust results for this mode for $D > 7$ unfortunately does not allow us to check the dependence of its quality factor on a_* for larger values of D. Nevertheless, a clear conclusion can be safely drawn when the two lowest multipole spinor modes are compared: the ''corotating'' modes with $m = 1/2$ are much better oscillators than the ''contra-rotating'' ones with $m = -1/2$.

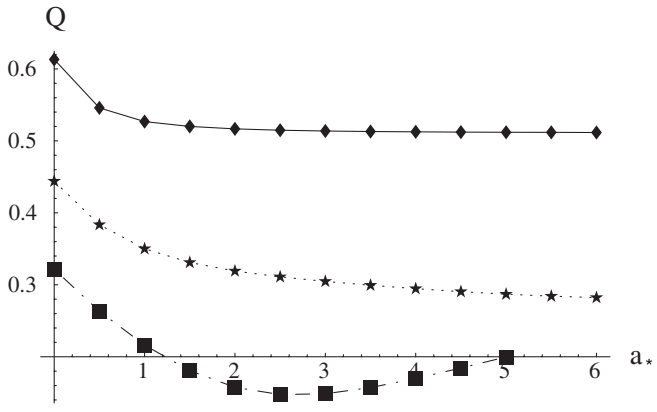

FIG. 5. Quality factor for the spinor field multipole mode ($\ell = 1/2$, $m = -1/2$), and for $D = 5$, 6, 7 (from top to bottom).

V. CONCLUSIONS

In this paper, we have performed a comprehensive study of the fundamental quasinormal modes of all Standard Model fields propagating on a brane embedded in a higher-dimensional rotating black-hole spacetime. The starting point of our analysis was the equations of motion for fields with spin $s = 0$, $1/2$ and 1 propagating on the induced-on-the-brane background, and their rewriting to the form of a Schrödinger-like, wave equation. By using numerical techniques, based on the continued fraction method, the quasinormal spectra of all species of fields were derived as a function of the black-hole angular momentum and dimensionality of spacetime.

The dependence of the QN spectra on the angular momentum of the black hole was found to be universal with both the real and (the absolute value of the) imaginary part of the QN frequency being suppressed as a_* increases. As a result, brane-localized fields propagating on the induced 4-dimensional background are longer-lived when the higher-dimensional black hole rotates faster. In addition, both $\omega_{\rm Re}$ and $\omega_{\rm Im}$ approach constant asymptotic values, as $a_* \to \infty$. These results hold for all species of fields, with the only exception arising for spinor fields with $m = -1/2$ and for $D \geq 7$. Figure 6 shows the collective behavior of all SM fields QN spectra as a function of a_*, for $D = 6$, and reveals the aforementioned spin-independent behavior.

In terms of the dimensionality of spacetime, our analysis confirmed the increase in the imaginary part of the QN frequency of all SM fields, as D increases, observed in the case of a nonrotating black hole [9]. The same behavior holds for arbitrary angular momentum of the black hole, a result that points to the conclusion that an increase in the number of transverse-to-the-brane dimensions reduces the lifetime of the field perturbations on the brane, in both spherically- and axially-symmetric backgrounds. With the exception again of spinor fields, $\omega_{\rm Im}$ tends again to a constant asymptotic value as $D \to \infty$. This behavior is clearly shown in Fig. 7, where the QN spectra of all SM fields are shown for $a_* = 1$. In the same figure, we also display the collective behavior of the real part of the QN frequency, $\omega_{\rm Re}$, as a function of D. This behavior is also

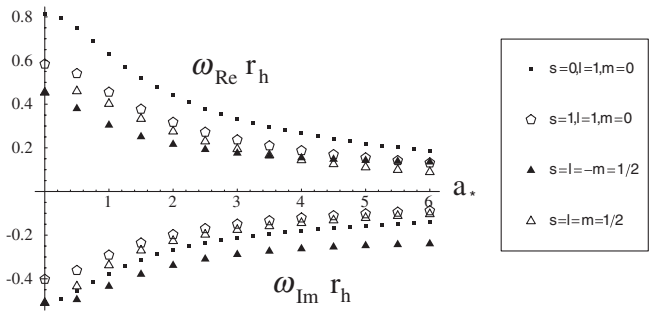

FIG. 6. Fundamental QN modes of fields with spin $s = 0$, $1/2$ and 1, for $D = 6$.

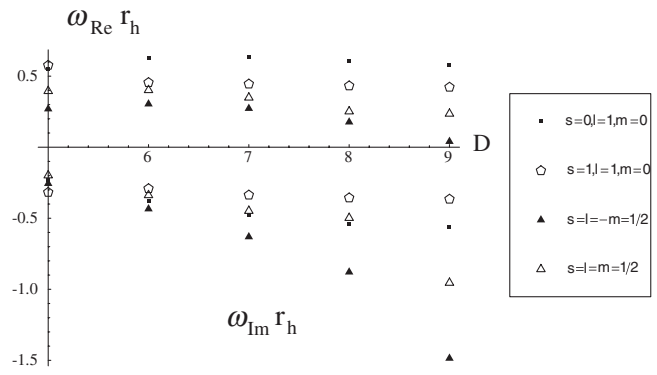

FIG. 7. Fundamental QN modes of fields with spin $s = 0, 1/2$ and 1, for $a_* = 1$.

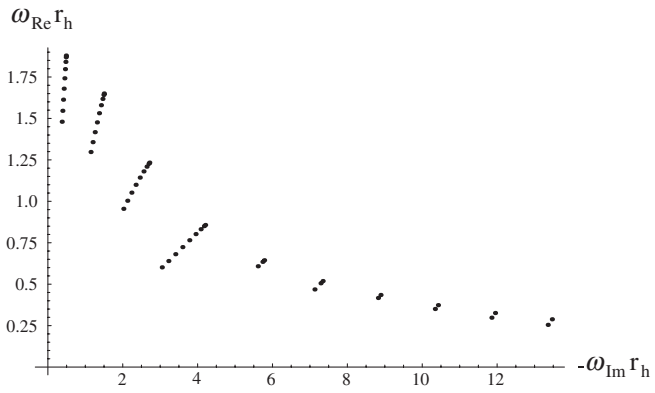

FIG. 8. A few higher overtones for the electromagnetic field mode ($\ell = 3$, $m = 0$), and $D = 6$.

found to be universal, with ω_{Re} increasing up to $D = 6$, in accordance with previously found results [9], but decreasing for higher values of D.

The quality factor Q, finally, that determines the best oscillator among the different field perturbations, was found to depend both on properties of the field, like its spin s or multipole numbers (ℓ, m), as well as on properties of the gravitational background, such as the dimensionality of spacetime and angular momentum of the black hole. The quality factor of modes with either $m = 0$ or $m > 0$ was found to decrease with D but (predominantly) increase with a_*. As a result, for all of these modes, Q takes its largest possible value for $D = 5$ and large a_*—among the different species, the fermionic modes were found to assume the largest value of Q for these parameter values. The situation however changes radically for modes with $m < 0$, whose quality factor is suppressed with D but also with a_*, rendering them worse oscillators than the ones with $m = 0$ or $m > 0$.

Being restricted by the standard model we did not compute quasinormal modes of massive fields, yet, as was shown in [27] for massive scalar and in [28] for massive vector fields, the QN spectrum can show rather exotic behavior, for instance, infinitely long living modes. Also, throughout this paper, we have restricted our study to the fundamental overtones ($n = 0$) of the QN spectra due to their dominance in the signal. Nevertheless, higher overtones of all SM fields with spin $s = 0, 1/2$ and 1 were also looked at in the context of our analysis. Their QN spectra were derived for the range $(0, r_h)$ of the angular momentum parameter a of the black hole with a step of $r_h/8$. In Fig. 8, we display a few of the higher overtones for a brane-localized gauge field with ($\ell = 3$, $m = 0$). For all higher overtones, it was found that an increase in a_* leads again to the decrease of the absolute values of both the real and imaginary parts of their QN frequencies.

We would like to finish our work with some important remarks. During our analysis, we made two simplifying assumptions. Firstly, our study was restricted to the case of higher-dimensional black holes with only one nonzero rotating parameter; that was due to the assumption that the colliding particles, that give rise to the black hole, were restricted to live on an infinitely-thin brane, and therefore had a nonvanishing impact parameter only along an axis parallel to the brane. In a more realistic case, where the brane is assumed to have a finite thickness—generically of the order of the fundamental length—the colliding particles can have nonzero impact parameters along the bulk directions, and thus give rise to a black hole with more than one rotating parameters. In more sophisticated brane-world models, that attack phenomenological problems like fast proton decay, large neutron-antineutron oscillations or FCNC, the quarks may be located at different 3-dimensional slices along the bulk and thus have, by construction, large separations along the bulk directions [29]. It seems therefore imperative that a more comprehensive study of higher-dimensional black holes, with all possible components of the angular momentum taken into account, need to be done in the future (for scalar particles in $D = 5$, the general equation of motion has been derived and shown to be separable in [30]). The second assumption made in our analysis was that the brane tension was much smaller than the mass of the produced black hole and thus it could be safely ignored. However, the ''friction'' between the black hole and the brane can alter the components of the angular momentum of the former [31], and excite brane degrees of freedom that could be interpreted as quasinormal modes. The analysis of such a realistic set-up, that would study the change in the spectrum of the quasinormal frequencies found here due to the brane-black-hole interaction, could also be the objective of a future work.

ACKNOWLEDGMENTS

P. K. acknowledges financial support from the U.K. Particle Physics and Astronomy Research Council (Grant Number PPA/A/S/2002/00350). The work of R. K. and A. Z. was supported by Fundação de Amparo à Pesquisa do Estado de São Paulo (FAPESP), Brazil.

[1] N. Arkani-Hamed, S. Dimopoulos, and G. R. Dvali, Phys. Lett. B **429**, 263 (1998); Phys. Rev. D **59**, 086004 (1999); I. Antoniadis, N. Arkani-Hamed, S. Dimopoulos, and G. R. Dvali, Phys. Lett. B **436**, 257 (1998).

[2] L. Randall and R. Sundrum, Phys. Rev. Lett. **83**, 3370 (1999); **83**, 4690 (1999).

[3] P. C. Argyres, S. Dimopoulos, and J. March-Russell, Phys. Lett. B **441**, 96 (1998); T. Banks and W. Fischler, Phys. Lett. B **441**, 96 (1998); S. B. Giddings and S. Thomas, Phys. Rev. D **65**, 056010 (2002); S. Dimopoulos and G. Landsberg, Phys. Rev. Lett. **87**, 161602 (2001).

[4] P. Kanti, Int. J. Mod. Phys. A **19**, 4899 (2004).

[5] H. P. Nollert, Class. Quant. Grav. **16**, R159 (1999).

[6] K. D. Kokkotas and B. G. Schmidt, Living Rev. Relativity **2**, 2 (1999).

[7] P. R. Brady, C. M. Chambers, W. G. Laarakkers, and E. Poisson, Phys. Rev. D **60**, 064003 (1999); B. Wang, E. Abdalla, and R. B. Mann, Phys. Rev. D **65**, 084006 (2002); V. Suneeta, Phys. Rev. D **68**, 024020 (2003); R. A. Konoplya, Phys. Rev. D **66**, 044009 (2002); A. Zhidenko, Class. Quant. Grav. **23**, 3155 (2006); J. x. Tian, Y. x. Gui, G. h. Guo, Y. Lv, S. h. Zhang, and W. Wang, Gen. Relativ. Gravit. **35**, 1473 (2003); C. Molina, D. Giugno, E. Abdalla, and A. Saa, Phys. Rev. D **69**, 104013 (2004); E. Abdalla, R. A. Konoplya, and C. Molina, Phys. Rev. D **72**, 084006 (2005); T. R. Choudhury and T. Padmanabhan, Phys. Rev. D **69**, 064033 (2004); M. Giammatteo and I. G. Moss, Class. Quant. Grav. **22**, 1803 (2005); V. Cardoso, R. Konoplya, and J. P. S. Lemos, Phys. Rev. D **68**, 044024 (2003); V. Cardoso, J. Natario, and R. Schiappa, J. Math. Phys. (N.Y.) **45**, 4698 (2004).

[8] G. T. Horowitz and V. E. Hubeny, Phys. Rev. D **62**, 024027 (2000); A. Nunez and A. O. Starinets, Phys. Rev. D **67**, 124013 (2003); V. Cardoso, O. J. C. Dias, and J. P. S. Lemos, Phys. Rev. D **67**, 064026 (2003); R. A. Konoplya, Phys. Rev. D **68**, 124017 (2003); C. Molina, Phys. Rev. D **68**, 064007 (2003); V. Cardoso, S. Yoshida, O. J. C. Dias, and J. P. S. Lemos, Phys. Rev. D **68**, 061503 (2003); V. Cardoso, J. P. S. Lemos, and S. Yoshida, J. High Energy Phys. 12 (2003) 041; Phys. Rev. D **69**, 044004 (2004); G. Siopsis, Phys. Lett. B **590**, 105 (2004); V. Cardoso, O. J. C. Dias, and J. P. S. Lemos, Phys. Rev. D **70**, 024002 (2004); R. A. Konoplya and E. Abdalla, Phys. Rev. D **71**, 084015 (2005); L. Vanzo and S. Zerbini, Phys. Rev. D **70**, 044030 (2004); J. Natario and R. Schiappa, Adv. Theor. Math. Phys. **8**, 1001 (2004); A. Lopez-Ortega, gr-qc/0605027; gr-qc/0605034.

[9] P. Kanti and R. A. Konoplya, Phys. Rev. D **73**, 044002 (2006).

[10] E. Abdalla, B. Cuadros-Melgar, A. B. Pavan, and C. Molina, gr-qc/0604033.

[11] E. Berti, K. D. Kokkotas, and E. Papantonopoulos, Phys. Rev. D **68**, 064020 (2003).

[12] R. C. Myers and M. J. Perry, Ann. Phys. (N.Y.) **172**, 304 (1986).

[13] P. Kanti and J. March-Russell, Phys. Rev. D **66**, 024023 (2002).

[14] P. Kanti and J. March-Russell, Phys. Rev. D **67**, 104019 (2003).

[15] J. N. Goldberg, A. J. MacFarlane, E. T. Newman, F. Rohrlich, and E. C. Sudarshan, J. Math. Phys. (N.Y.) **8**, 2155 (1967).

[16] E. Newman and R. Penrose, J. Math. Phys. (N.Y.) **3**, 566 (1962).

[17] S. Chandrasekhar, *The Mathematical Theory Of Black Holes* (Oxford University Press, Oxford, 1992).

[18] D. Ida, K. y. Oda, and S. C. Park, Phys. Rev. D **67**, 064025 (2003); **69**, 049901(E) (2004).

[19] S. A. Teukolsky, Phys. Rev. Lett. **29**, 1114 (1972); Astrophys. J. **185**, 635 (1973).

[20] U. Khanal, Phys. Rev. D **28**, 1291 (1983).

[21] H. Suzuki, E. Takasugi, and H. Umetsu, Prog. Theor. Phys. **100**, 491 (1998).

[22] E. W. Leaver, Proc. R. Soc. A **402**, 285 (1985).

[23] A. Rostworowski, gr-qc/0606110.

[24] B. F. Schutz and C. M. Will, Astrophys. J. Lett. **291**, L33 (1985); S. Iyer and C. M. Will, Phys. Rev. D **35**, 3621 (1987); R. A. Konoplya, Phys. Rev. D **68**, 024018 (2003); J. Phys. Stud. **8**, 93 (2004).

[25] K. D. Kokkotas and B. F. Schutz, Phys. Rev. D **37**, 3378 (1988); V. Ferrari, M. Pauri, and F. Piazza, Phys. Rev. D **63**, 064009 (2001); R. A. Konoplya, Gen. Relativ. Gravit. **34**, 329 (2002); Phys. Rev. D **66**, 084007 (2002); S. Fernando and C. Holbrook, hep-th/0501138; A. Zhidenko, Class. Quant. Grav. **21**, 273 (2004); R. A. Konoplya and A. Zhidenko, J. High Energy Phys. 06 (2004) 037.

[26] C. M. Harris, hep-ph/0502005.

[27] L. E. Simone and C. M. Will, Class. Quant. Grav. **9**, 963 (1992); R. A. Konoplya, Phys. Lett. B **550**, 117 (2002); A. Ohashi and M. Sakagami, Class. Quant. Grav. **21**, 3973 (2004); R. A. Konoplya and A. V. Zhidenko, Phys. Lett. B **609**, 377 (2005).

[28] R. A. Konoplya, Phys. Rev. D **71**, 024038 (2005).

[29] D. C. Dai, G. D. Starkman, and D. Stojkovic, Phys. Rev. D **73**, 104037 (2006).

[30] V. P. Frolov and D. Stojkovic, Phys. Rev. D **67**, 084004 (2003).

[31] V. P. Frolov, D. V. Fursaev, and D. Stojkovic, J. High Energy Phys. 06 (2004) 057; Class. Quant. Grav. **21**, 3483 (2004).